

RETINAL DISEASE PREDICTION USING LEAKY RECTIFIED LINEAR UNIT BASED GATED RECURRENT UNIT MODEL

JYOTHIRMAI JOSHI^{1*}, MALINI MUDIGONDA², RAGHAVA MORUSUPALLI³

^{2,3}Department of Biomedical Engineering, Osmania University, Hyderabad, Telangana, India

¹VNR Vignan Jyothi Institute of Engineering and Technology, Hyderabad, Telangana

³Department of Computer Science engineering, CVR College of Engineering, Hyderabad, Telangana, India

Corresponding Author: Jyothirmai_j@vnrvjiet.in

ABSTRACT

Detecting retinal disease has become more difficult in recent years, attracting a lot of attention. However, when predicting retinal disease, problems has caused due to a lack of a thorough understanding of all components in disease progression. The complexity and variability of retinal diseases can also have an impact on prediction accuracy. In this research, a Leaky Rectified Linear Unit (ReLU)-based Gated Recurrent Unit (GRU) classification model is suggested to improve retinal disease detection accuracy. Data is obtained from the Retinal Optical Coherence Tomography (OCT) image and the Noor Eye Hospital dataset. The preprocessing is then done by using Minmax normalization techniques. Additionally, the Local Ternary Pattern and Gray Level Co-occurrence Matrix (GLCM) are used to identify and select the relevant features from the raw data. Next, the tournament-based Levy Multiverse Optimization Algorithm (LMOA) feature selection is used to improve model performance by identifying relevant features. Finally, ReLU-based GRU classification was used to improve accuracy in retinal eye disease. According to the results, the proposed technique attained a higher accuracy of 99.01% in the OCT image dataset and 99.59% accuracy on the Noor Eye dataset, which was greater than the existing approaches.

Keywords: *Age-related Macular Detection, Choroidal Neo-Vascularization, Gated Recurrent Unit, Leaky Rectified Linear Unit, Optical Coherence Tomography.*

1. INTRODUCTION

In recent years, the field of retinal disease prediction has seen significant advancements. Researchers and healthcare professionals have developed sophisticated Machine Learning (ML) algorithms and Artificial Intelligence (AI) based models to detect and predict various retinal diseases, such as age-related macular degeneration, diabetic retinopathy, and glaucoma [1]. These AI systems analyze retinal images obtained through imaging techniques and can accurately identify early signs of these diseases, enabling early interference and potentially preventing vision loss or other complications. The integration of AI in retinal disease prediction has the potential to transform eye care and improve patient results worldwide [2]. The process of retinal disease prediction involves several steps. First, retinal images are obtained using generalized imaging methods, such as Optical Coherence

Tomography (OCT) [3,4]. These images were pre-processed to enhance their quality and remove the noise. Next, ML algorithms or AI models are trained using a large dataset of annotated retinal images. These models learn to recognize patterns and features associated with different retinal diseases by analyzing the labeled data. During the prediction phase, the trained AI model is presented with new, unseen retinal images [5]. The images are tested by the AI model, which contrasts them with the patterns during the training process. Based on these comparisons, the model can make predictions about the presence of retinal diseases in their development. The accuracy of the predictions is continually validated and refined through feedback and updates to the AI model. This iterative process helps improve the model's performance and ensures its reliability in real-world clinical backgrounds [6,7].

The Leaky ReLU-based Gated Recurrent Unit (GRU) is a novel approach for retina disease prediction that has the benefits of both Leaky ReLU and the GRU architecture. The Leaky ReLU activation function introduces a small, non-zero slope for negative inputs, preventing the vanishing gradient problem and enabling better information flow during training [8,9]. This non-linearity enhances the model's ability to capture complex patterns in retinal data. Incorporating Leaky ReLU within the GRU, an advanced type of recurrent neural network, facilitates effective sequential modeling of temporal dependencies in retinal images [10,11]. The GRU's mechanism enables the model to remove noise and enhance its ability to manage sequences of different lengths effectively. By training the Leaky ReLU-based GRU on a large dataset of retinal images with associated disease labels, the model can learn to recognize refined pointers and patterns indicative of different retina diseases [12]. This predictive capability holds the potential for early diagnosis and proactive treatment of retinal conditions, eventually improving patient outcomes and quality of life. Overall, the combination of Leaky ReLU-based GRU offers a powerful and interpretable framework for accurate retina disease prediction [13]. However, Limited and low-quality data, class imbalance, interpretability of predictions, manual annotation challenges, defining detailed ground truth, and limited clinical labels are the main problems faced during retinal disease prediction [14,15]. To solve the issues in retinal disease prediction, a Leaky ReLU-based GRU was suggested to improve length sequences effectively and enhance model interpretability. This combination aims to provide accurate predictions, handle limited data, and helps clinicians in making informed decisions for early diagnosis and treatment.

The contribution of the research, are listed as follows;

- In this research, a Leaky Rectified Linear Unit (ReLU) based Gated Recurrent Unit (GRU) model is proposed to predict the retinal disease.
- The input images are obtained from retinal OCT and Noor Eye Hospital datasets, where normalization is applied to facilitate the classification of retinal features.
- The LMOA feature selection method is introduced to address dimensionality concerns and effectively extract the most

relevant information from the features obtained.

The rest of the research are structured as follows: Section 2 describes the Literature survey in this field, while Section 3 describes the proposed methodology. Sections 4 and 5 described the overall results and conclusions.

2. LITERATURE SURVEY

In this research, literature survey was utilized to examine the problems related to predicting retinal diseases in the existing methods. The survey involved gathering and analyzing information from various published works to identify the challenges, and areas for improvement in the field of retinal disease prediction. This process helps to understand the issues with existing approaches and potentially develop better methods for predicting retinal diseases.

Toğaçar et al. [16] developed an AI-based Slime Mold Algorithm (SMA) for retinal disease detection. The utilization of the SMA optimization method involved selecting the most prominent activations from the sets of activations acquired through CNN models using the training data. This stands in contrast to the time-consuming process of manually reviewing OCT images, this proposed approach enables the execution of multiple procedures rapidly. However, the suggested approach can cause increased training costs, and it is essential to conduct clinical validation in the experimental analysis to determine its effectiveness and reliability.

Alqudah et al. [17] developed a Diabetic Macular Edema (DME) for multiclass classification of eye retina diseases. The CNN architecture aims to capture advanced features from OCT images. By subjecting the input OCT image to a variety of filters, a feature map is generated. Visualizations of the features from each convolutional layer were provided to enhance comprehension of the model's design. However, the suggested method needs to be analyzed with activation layers for both test scenarios and adversarial situations for the decision-making process.

Xu et al. [18] suggested a Convolution Neural Network (CNN) to identify the various retinal layers extracting useful information. This combined approach effectively captures essential features in both the channel and spatial dimensions of retinopathy images, mitigating the adverse

influence of background information on classification outcomes. The suggested method significantly helps the network in focusing on extracting retinopathy areas and enhances its adaptability to various datasets. However, due to these advancements, the test results did not exhibit substantial improvements, indicating that the network may still possess certain limitations in achieving significant performance gains.

Liew et al. [19] introduced a novel approach called Multi-Size Kernels ξ cho-Weighted Median Patterns (MSK ξ MP) for predicting muscular retinal diseases. This method effectively encodes textural patterns at both local and regional scales, leading to enhanced edges in different directions and effective suppression of speckle noise. Consequently, the proposed method demonstrates high specificity, instilling significant confidence in the accurate identification of true negatives during the classification process. However, selecting a median value without incorporating any weights from a high noise-density image raises practical concerns about the suggested method.

Kim and Tran [20] implemented DL models for the categorization of OCT images into four classes, utilizing binary CNN classifiers. The methodology included amalgamating the outputs of either three or four binary CNN classifiers to predict the outcomes. This method has the enhanced effectiveness of employing multiple binary classifiers in contrast to utilizing multi-class classifiers. To address overfitting problems, the suggested method incorporated two dropout layers. However, for further enhancement in classification accuracy, there is a necessity to explore new architectures for the deep learning model and consider the integration of handcrafted features in the analysis.

The proposed method aims to address the limitations found in existing retinal prediction approaches. By enhancing data quality and eliminating inconsistencies, the suggested approach aims to significantly improve the accuracy and reliability of classification models.

3. PROPOSED METHOD

To address the challenges in the existing methods such as energy consumption, time delay, etc. the suggested Leaky ReLU-based GRU was utilized to improve the accuracy. The objective of the proposed method is to enhance the accuracy of retinal disease prediction. The suggested Leaky

ReLU improves the depth of network architectures, enabling better feature representation, while GRU effectively captures sequential dependencies from the selected features. The process involves various stages of classifying the retinal disease which are data collection, pre-processing, feature extraction, feature selection, and classification. The flow diagram of the proposed method is illustrated in Figure 1.

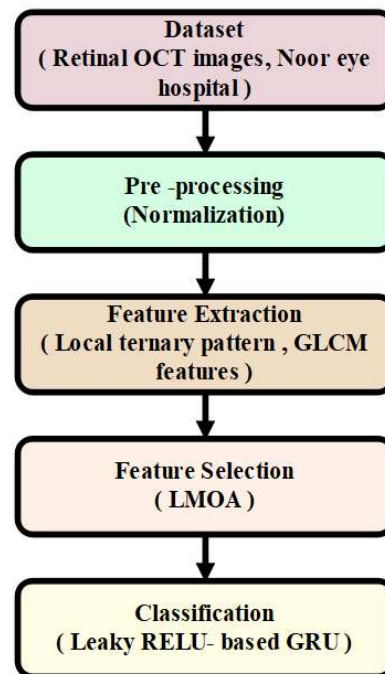


Figure 1. Flow diagram of the suggested method

3.1. Dataset collection

Datasets are essential for training, validating, and testing proposed methods that enable algorithm development for a better understanding of method behavior. In this research, the raw data is obtained from publicly available datasets such as the Retinal Optical Coherence Tomography (OCT) [20] dataset and the Noor Eye Hospital dataset (NEH) [17]. Retinal OCT images provide high-resolution cross-sectional views of retinal layers, helping accurate disease diagnosis. The Noor Eye Hospital dataset offers diverse real-world cases, enhancing the model's ability to predict various retinal conditions effectively. The description of the mentioned dataset is as follows:

- **Retinal OCT images dataset:** The Optical Coherence Tomography (OCT) dataset for retinal diseases is employed to acquire high-resolution cross-sectional views of live

subject's retinas. Roughly 30 million OCT scans are conducted annually, and the interpretation and analysis of these images constitute a substantial time-consuming process. Evaluating the efficacy of the integrated coherent convolutional neural network on this dataset and its capacity to generalize from the internet-sourced data accessible on Kaggle is dominant. These methodologies enhance the network's flexibility and its ability for precise classification across diverse conditions within OCT images. The experimentation involved utilizing a set of 8,000 images encompassing distinct categories, including DME, DMD, and normal images.

- **NEH dataset:** The subsequent dataset originated from the Noor Eye Hospital (NEH) Dataset, encompassing 148 SD-OCT volumes (comprising 48 AMD, 50 DME, and 50 Normal cases). These volumes were captured utilizing the Heidelberg SD-OCT imaging system at NEH in Tehran. Within each volume, there were 19 to 61 B-scans, each with a resolution of $3.5 \mu\text{m}$, and the scanning area measured $8.9 \times 7.4 \text{ mm}^2$.

The suggested dataset has faced issues such as noise, inconsistent lighting, and artifacts. Pre-processing technique normalization is utilized to improve data quality by enhancing accuracy and reliability in prediction.

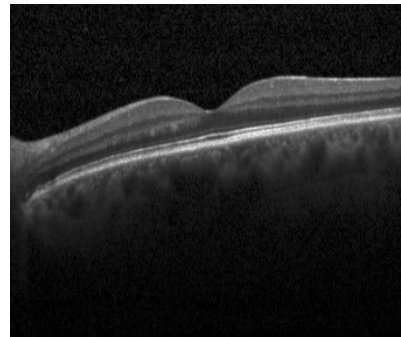
3.2. Data pre-processing

After data acquisition, the pre-processing stage is conducted to transform the data into a processed format, free from complexities. The process involved removing noisy and unwanted portions from the images using normalization techniques. The preprocessing is performed by normalization technique on input images of normal, AMD, and DME where the noises from those images are removed, thus resulting in normalized retinal images. Each image was normalized by using Min-Max normalization technique. The retinal fundus images have noise, blur, and low contrast because of complex imaging. Using the normalization technique, the noisy elements are removed, thus resulting in normalized retinal images which are given as input for feature extraction. The normalization process transformed the n-dimensional grayscale image, which was originally represented by intensity values in the range of (Min, Max), into a new image with intensity values now ranging and confined within the range of (0, 1). The calculation

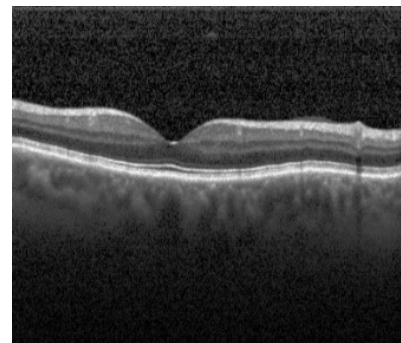
for determining the min_max limits is represented by Equation (1).

$$v^1 = \frac{v - \min(A)}{\max(A) - \min(A)} (new_{\max(A)} - new_{\min(A)}) + new_{\min(A)} \quad (1)$$

The dataset-A's minimum value is denoted as $\min(A)$, and its maximum value is denoted as $\max(A)$. The initial value is represented as v , and the updated value is v^1 . The boundary values for the new minimum and maximum are within the ranges of $new_{\min(A)}$ and $new_{\max(A)}$ respectively. This ensures balanced feature extraction, where methods like GLCM and LTP analyze patterns with equal relevance. The normalized inputs enhance the accuracy and reliability of extracted features, improving subsequent disease prediction outcomes. Figure 2 illustrates the normalization pre-processing images of the Retinal OCT and Noor eye hospital datasets.



(a)



(b)

Figure 2. Pre-processed images

3.3. Feature Extraction

The pre-processed output obtained from the initial stage is then fed into the subsequent feature extraction phase. The feature extraction aims to identify and select the most informative and relevant attributes from the raw data, which plays

a vital role in improving the performance of various applications like machine learning and pattern recognition algorithms. In this context, the Local Ternary Pattern and Gray Level Co-occurrence Matrix (GLCM) [21] features approach were briefly described below.

- **Local ternary pattern:**

The discriminative power of the Local Ternary Pattern (LTP) is utilized to analyze the texture of the image, along with the Local Binary Pattern (LBP) effectively reduces the influence of illumination and noise in the image. The LTP method is evaluated to the green (G), red (R), and blue (B) colour channels allowing for texture analysis. Employing multi-scale sampling in the classification texture algorithm proved to be efficient, and the dimensions were effectively reduced through the application of LTP. The measurement of the LTP is computed using Equation (2).

$$s^l(g_c, g_p, \delta) = \begin{cases} +1, & g_p - g_c > \delta \\ 0, & |g_p - g_c| \leq \delta \\ -1, & g_p - g_c < -\delta \end{cases} \quad (2)$$

The formula's output (+1, 0, or -1) can correspond to the presence of specific textural characteristics related to different retinal conditions. By applying such decision rules to the differences in pixel intensities, it can be able to highlight specific textural features associated with retinal diseases. For retinal disease prediction, inputs in LTP and GLCM methods encompass retinal images. LTP characterizes texture via pixel relations, while GLCM quantifies pixel intensity patterns. These features aid in detecting disease-related patterns for accurate prediction. In this context, the empirical thresholding is denoted by δ , the grayscale intensity of the central pixel is represented by g_c , and g_p represents the p-th term sampling point of the estimated intensity.

- **Grey Level Co- co-occurrence matrix (GLCM)**

The statistical GLCM method is employed to quantify the spatial relationships between pixels within the image. By evaluating the presence of specific pixel pairings with particular values in the image, a GLCM is created, where G represents the image's grey levels. The ratio of the two pixels with the matrix element $\frac{P(i,j)}{\Delta_x \Delta_y}$, where (Δ_x, Δ_y) is the pixel's separation distance. The matrix elements were obtained by evaluating the statistical

probability values of second-order changes in grey levels occurring at a specific angle and displacement distance of $\frac{P(i,j)}{d,\theta}$. GLCM is a widely used method for analyzing textures in images. The statistical GLCM method is used to measure the spatial relationship between the pixels of the image. By evaluating the spatial relationship and pixel pairings with certain values that exist in an image is identified. The first and second-order features are extracted using GLCM with various intensities including the Contrast, Correlation, Homogeneity, Energy, Sum average, Entropy, Variance, Sum entropy, Difference variance, Sum Variance, Information measure of correlation-1, Difference entropy and Information correlation-2.

By combining LTP and GLCM helps to enhance the accuracy of predictive models for identifying retinal diseases more effectively. Hence, the GLCM and LTP were presented for extracting the features and the features extracted from the Retinal OCT images resulted in a length of feature 560 and the Noor, eye hospital images resulted in a length of feature 560. These techniques can enhance the discriminative power of the extracted features, helping in accurate disease prediction. The GLCM and LTP methods generate texture and intensity features from inputs like retinal images. Furthermore, the extracted features such as shape, color, and size from the normalized retinal images are given as input to the feature selection process to select optimal features for precise classification.

3.4. Feature selection

After the feature extraction stage, the feature selection process is performed using extracted features from the normalized retinal images for accurate classification. Feature selection is crucial to enhance model efficiency, reduce overfitting, and improve interpretability. In this stage, the tournament-based Levy Multiverse Optimization Algorithm (LMOA) is introduced for efficient feature selection, resulting in improved overall performance. Because MOA has different downgrades such as less classification accuracy, local optima, and less convergence. Hence the LMOA is presented in this research to select the optimal features from the extracted features. This process more effectively identifies the highest fitness function value, which is then chosen for updating the subsequent generation. In the LMOA, the location update is achieved by incorporating the mutation factor during the screening process. This adaptation improved the global and local

optimization, effectively striking a better balance between exploitation and exploration algorithms. The equation appears to be a combination of various statistical and mathematical concepts, potentially used in a predictive model. The convergence speed is improved using the LMOA optimization algorithm and convergence of the optimal solution. Equation (3) describes the mathematical model of the Levy. These factors could be represented by the variables μ , σ , and v , and the equation can be designed to capture the relationships and interactions between the factors. As a result, the convergence speed of the optimization algorithm is enhanced, leading to the convergence of the optimal solution.

$$Levy(\lambda) = 0.01 \times \frac{\mu \times \sigma}{|v|^{\beta}} \quad (3)$$

Where the v and μ obey the normal distribution which is represented in the equation represents the standard deviation measurement. β represents a constant exponent that modifies the effect of the denominator on the equation's result. Equations (4) and (5) represents the standard deviation measurement.

$$\lambda = \beta + 1$$

Then,

$$\mu \sim N(0, \sigma^2), v \sim N(0, \sigma_v^2) \quad (4)$$

$$\sigma = \left[\frac{r(1+\beta) \times \sin\left(\frac{\pi\beta}{2}\right)}{r\left(\frac{1+\beta}{2}\right) \times \beta \times 2^{\left(\frac{\beta-1}{2}\right)}} \right]^{\frac{1}{\beta}} \quad (5)$$

Where $\sigma_{v=1}$ and the β is the parameter for controlling which will vary based on the density function. The step length is calculated as Equation (6):

$$s = \frac{\mu}{|v|^{\beta}} \quad (6)$$

In Equation (6), the step length is determined by measuring the initial and final points of each step. The integration of Tournament selection in LMOA helped to minimize and address local optimization problems. The fitness function is instrumental in converting the present position to a locally optimal position. To achieve efficiency in results and fitness function, the relevant features were summarized into a single content. In optimization algorithms, a fitness function is a

crucial component. The fitness function defines how well a potential performs with respect to the optimization problem to solve. The goal of optimization is to find the best solution, which often corresponds to the maximum or minimum value of the fitness function. The purpose of the fitness function is to quantify the quality of solutions to make decisions about which solutions to explore and which to remove. The fitness function played a crucial role in yielding optimal solutions, with X represented as the row vector and y as the argument, as calculated using Equation (7).

$$y = 100 \times (X(1)^2 - X(2))^2 + (1 - X(1))^2 \quad (7)$$

In LMOA, the inclusion of a mutation factor served to preserve population diversity and mitigate premature convergence. The selected feature consists of a length of 213 for retinal OCT images and 256 for Noor eye hospital images. The related features are summarized into single content for efficient results and fitness function. Hence, LMOA feature selection based on tournament methodology identifies the most informative and distinctive features of GLCM. This augmentation improves the analysis of pattern recognition within the realm of image processing and computer vision applications. The optimized LMOA algorithm selects the optimal features from the LTP-GLCM's extracted features. Additionally, the optimization problems have been resolved by using the LMOA, thus resulting in high accuracy. Finally, the selected optimal features from the extracted features, using LMOA are given as input to Leaky RELU – based GRU for precise classification.

3.5. Classification using Leaky RELU – based GRU

After the stage of feature selection, the proposed Leaky RELU- based GRU is performed by utilizing the Retinal OCT and NEH dataset to improve the accuracy in retinal disease classification is briefly described below;

3.5.1. Gated Recurrent Unit

GRU was considered as variants of Recurrent Neural Networks (RNN) and were commonly utilized to address sequence of -related challenges. In contrast to LSTM, GRU replaces LSTM's, input gate forget gate and output gate with the update gate Z_t and the reset gate r_t . While ensuring that GRU's prediction accuracy is not inferior to that of LSTM, the reduction of training parameters

enables faster divergence speed. The architecture of GRU were described in Figure 3.

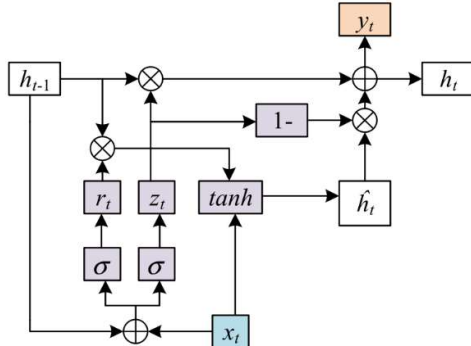


Figure 3. Structure of Gated Recurrent Unit

The reset gate r_t automatically manages the combination of previous memory with new input while the update gate Z_t determines the volume of previous memory retained at the present step. A higher value of Z_t allows for more data from the previous stage to be preserved in the current memory. Conversely, a smaller amount of r_t results in the forgetting of more state data from the previous stage. In the initial step, Z_t and r_t are computed based on the input data x_t at the present stage and the hidden layer data h_{t-1} retained from the earlier time stage. Next, the step involves utilizing the reset gate was decide the amount of data stored in the node. Finally, hidden layer output at the current time step is calculated using the update gate. The following equations illustrated the mathematical process of the GRU is illustrated in Equations (8-11).

$$Z_t = \sigma(W_z x_t + U_z h_{t-1} + b_z) \quad (8)$$

$$r_t = \sigma(W_r x_t + U_r h_{t-1} + b_r) \quad (9)$$

$$\hat{h}_t = \tanh(W_h x_t + U_h (r_t \otimes h_{t-1}) + b_h) \quad (10)$$

$$h_t = (1 - z_t) \otimes h_{t-1} + Z_t \otimes \hat{h}_t \quad (11)$$

Where, σ determines the functions of sigmoid; W_z, W_r, W_h, U_z, U_r and U_h are weight matrices; b_z, b_r, b_h are the biased results; \hat{h}_t is the input state of the sum x_t and the h_{t-1} is the hidden layer in the previous stage h_t is the hidden layer output, \otimes describes Hadamard product.

GRUs are a type of RNN architecture commonly used for sequence modeling. Leaky ReLU is an activation function used in neural networks. While GRUs and Leaky ReLU serve different purposes, there are some challenges such

as the vanishing gradient problem and memory retention in GRUs that Leaky ReLU could potentially address in specific cases. Leaky ReLU can be used as an activation function within the GRU's gates or hidden states, but its effectiveness would depend on the specific problem. In GRU classification for retinal disease prediction, sequential data is often used. The input data consists of sequences of retinal image information, allowing the GRU model to capture temporal patterns and dependencies for accurate disease prediction over time.

3.5.2. Activation function of Leaky – ReLU

An activation function is a mathematical function used in neural networks to introduce non-linearity and enable the model to learn complex patterns and solve a wide range of problems effectively. The default activation function in a GRU is the hyperbolic tangent (tanh) function for the update and reset gates and the sigmoid function for the output gate. These activations help control the flow of information and the memory update within the GRU. However, the default activation function in a GRU (tanh) can suffer from the vanishing gradient problem, which can delay the method capacity to learn long-term needs in sequential data due to diminishing gradients during training. However, when dealing with bearing signals, ReLU's rounding off characteristics for negative inputs which can lead to weakened model recognition performance for bearing performance degradation. To overcome this limitation, Leaky ReLU is employed in this research to tackle the problem arising from negative inputs. Additionally, a dropout region is introduced to improve the model's capability and reduce joint adaptability among neural nodes, serving as data augmentation to mitigate overfitting. As a result, ReLU is replaced by the Leaky ReLU function, and incorporated to achieve these enhancements in the model. The algorithm is as follows in Equations (12-14).

$$LReLU(Z_i^l) = \max(a_i Z_i^l, Z_i^l) \quad (12)$$

$$r_i \sim \text{Bernoulli}(p) \quad (13)$$

$$c_i^l = r_i * LReLU(Z_i^l) \quad (14)$$

The $LReLU(\cdot)$ represents Leaky ReLU, where a_i denotes semi-axis of negative slope of the LReLU. The vector r_i comprises numerous independent variables following the same Bernoulli distribution, and p describes the

possibility of neuron failure c_i^l . The activation of Z_i^l is denoted as c_i^l .

3.5.3. Process of GRU with Leaky ReLU

The process of Leaky ReLU and GRU in retinal disease classification models enhances feature extraction and temporal analysis. Leaky ReLU improves the depth of network architectures, enabling better feature representation, while GRU effectively captures sequential dependencies from the selected features. This combined approach offers the potential to achieve higher accuracy in retinal disease prediction. It comprises multiple gates responsible for regulating the flow of information within the cell. The essential gates in a GRU cell are the update gate (z) and the reset gate (r), which dictate the retention of the previous hidden state and the integration of new information, respectively:

- **Update Gate (z):** The update gate is calculated using a sigmoid activation function, similar to the standard GRU cell.
- **Candidate Hidden State (~h):** In this adapted version, the candidate hidden state is obtained by applying a leaky ReLU activation to the sum of the input and the reset gate. This addition of the leaky ReLU activation introduces non-linearity, enhancing the model's ability to capture complex patterns within the candidate's hidden state.
- **Reset Gate (r):** The reset gate is calculated by applying a sigmoid activation function to the combination of the input and the previous hidden state, as in the standard GRU cell.
- **Hidden State (h):** The new hidden state is calculated by combining the previous hidden state and the candidate hidden state, weighted by the update gate, as in the standard GRU cell.

The parameters were addressed within the GRU architecture through the incorporation of update and reset gates in the gating mechanism, which takes inputs from the RNN x_t, h_{t-1} and generates \hat{h}_t . The Leaky ReLU activation function is applied element-wise to the linear transformations in the equations. Here, the GRU with Leaky ReLU activation function is illustrated in Equations (15-18).

Update Gate (Z_t) with Leaky ReLU:
 $Z_t = \text{sigmoid}(W_t * [h_{t-1}, x_t] + b_z)$ (15)

Reset Gate (r_t) with Leaky ReLU:
 $r_t = \text{sigmoid}(W_t * [h_{t-1}, x_t] + b_r)$ (16)

Candidate Hidden state (\hat{h}_t) with Leaky ReLU:
 $\hat{h}_t = \text{tanh}(W_h * [r_t * h_{t-1}, x_t] + b_h)$ (17)

Hidden State (h_t) update:

$$h_t = (1 - z_t) * h_{t-1} + z_t * (\hat{h}_t * \text{leaky}_{relu}(W_{hh} * h_{t-1}) + b_{hh})$$
 (18)

Where, leaky_{relu} Is the Leaky ReLU activation function applied element-wise x_t is the input at time step 't'. h_{t-1} is the previous hidden state at time step $t - 1$. W_z, W_r and W_h are weight matrices for the update gate, rest gate and candidate hidden stage. b_z, b_r and b_h are the bias terms for update gate, rest gate and candidate hidden state respectively. W_{hh} and b_{hh} are the weight matrix and bias terms for the hidden state passed through the reset gate. Hence, existing activations, like the default tanh in GRU, provide bounded output of symmetric handling for positive and negative values. However, Leaky ReLU overcomes the vanishing gradient issue by introducing a small, non-zero slope for negative inputs, thus preventing "dying ReLU" problem and enabling better learning of negative values. Leaky ReLU's simplicity and effectiveness in handling negative inputs make it a popular choice in deep learning models, enhancing the learning of complex patterns and improving the overall performance of the model. Hence, the Leaky ReLU based GRU has addressed the limitations found in the classification for retinal prediction approaches.

4. RESULTS AND DISCUSSIONS

This section focuses on evaluating the results of the proposed method for Retinal disease detection. It is divided into two subsections: performance analysis and comparative analysis. In the performance analysis, it assesses the efficiency of the proposed approach using Retinal OCT images from the Noor eye hospital dataset. To validate the model's performance, it utilizes key parameters such as accuracy, sensitivity, specificity, Matthews Correlation Coefficient (MCC), and error rate. These metrics are calculated using Equations (19 -23) respectively.

$$\text{Accuracy} = \frac{TN+TP}{TN+TP+FP+F}$$
 (19)

$$\text{Sensitivity} = \frac{TP}{FN+TP}$$
 (20)

$$Specificity = \frac{TN}{TN+} \tag{21}$$

$$MCC = \frac{TN \times TP - \times FN}{\sqrt{(TP+FP) \times (FP+TN) \times (FN+TP) \times (FN+TN)}} \tag{22}$$

$$Error\ rate = \frac{FP}{FP+} \tag{23}$$

4.1. Experimental setup

The Leaky ReLU-based GRU achieves effective results, and its performance is validated on the MATLAB R2020b software environment, running on a Windows 10 operating system with 16 GB Random Access Memory and an Intel i7 processor. The efficient MCC metric, which ranges between 0 and 1, represents the agreement between the predicted and actual values, with 0 indicating no agreement and 1 indicating perfect agreement. The evaluation of the OCT dataset includes assessing ML models for diabetes prediction and exploring Actual Features, Optimized Features, and Different Optimization algorithms to enhance effectiveness. These

findings provide valuable insights for healthcare applications and contribute to the improvement of retinal eye disease management.

4.2. Performance analysis of Retinal OCT images dataset

In this subsection, it evaluates the performance of the suggested approach utilizing various methods, containing, Neural Network (NN), Generative Adversarial Network (GAN), Recurrent Neural Network (RNN) and Leaky ReLU-GRU. The evaluation is conducted on the OCT images dataset, and results are represented in Table 1, Table 2, Table 3 and Table 4. Table 1 represents the value obtained from the suggested method in OCT images dataset for Actual Features while Table 2 represents the Optimized features. Table 3 represents the Different optimization algorithms. Table 4 represents the Different activation function. The performance analysis of OCT images dataset for Actual features is illustrated in Table 1.

Table 1. Performance Analysis Of OCT Images Dataset For Actual Features

Actual Features	Accuracy	Sensitivity	Specificity	MCC	Error-rate
NN	88.27	88.09	89.08	86.77	11.73
GAN	90.91	88.87	91.89	87.60	9.09
RNN	87.73	87.24	89.87	85.48	12.27
LeakyRELU-GRU	95.81	94.93	93.63	94.44	4.19

The results from Table 1 demonstrate that the proposed method serves as an excellent classifier for distinguishing retinal patients in the OCT dataset. The performance of the suggested

classification methods outperforms the existing model in terms of overall metrics, particularly in accuracy of 95.81% respectively.

Table 2. Performance Analysis Of OCT Images Dataset For Optimized Features

Optimized features	Accuracy	Sensitivity	Specificity	MCC	Error-rate
NN	90.51	91.48	88.85	91.94	9.49
GAN	92.30	91.86	92.91	90.77	7.70
RNN	89.53	90.96	91.81	89.85	10.47
LeakyRELU-GRU	99.01	99.16	98.08	99.20	0.99

The results from Table 2 demonstrate that the proposed method serves as an excellent classifier for distinguishing retinal patients in the OCT dataset. The performance of the suggested classification methods outperforms the existing model in terms of overall metrics, particularly in accuracy of 99.01% respectively. Table 3 evaluates the performance evaluation of the suggested approach utilizing various methods, including, Particle Swarm Optimization (PSO), Ant Colony Optimization (ACO), Artificial Bee

Colony (ABC) and Leaky ReLU-GRU. The evaluation is conducted on the OCT images dataset.

The results from Table 3 demonstrate that the proposed method serves as an excellent classifier for distinguishing retinal patients in the OCT dataset. The performance of the suggested classification methods outperforms existing model in terms of overall metrics, particularly in accuracy of 99.81% respectively.

Table 3. Performance Analysis Of OCT Images Dataset For Different Optimization Algorithms

Optimization methods	Accuracy	Sensitivity	Specificity	MCC	Error-rate
PSO	92.73	90.95	91.75	93.89	7.27
ACO	94.82	93.98	91.52	92.20	5.18
ABC	96.41	94.92	95.83	93.73	3.59
Proposed	99.01	99.16	98.08	99.20	0.99

Table 4. Performance Analysis Of OCT Images Dataset For Different Activation Functions

Activation functions	Accuracy	Sensitivity	Specificity	MCC	Error-rate
Sigmoid	92.73	91.90	91.81	93.70	7.27
RELU	97.19	96.73	95.78	95.37	2.81
Tanh	94.61	93.42	91.89	92.76	5.39
LeakyRELU-GRU	99.01	99.16	98.08	99.20	0.99

The results from Table 4 demonstrate that the proposed method serves as an excellent classifier for distinguishing retinal patients in the OCT dataset. The performance of the suggested classification methods outperforms the existing model in terms of overall metrics, particularly in accuracy of 99.01% respectively.

4.3. Performance analysis of Noor Eye Hospital dataset

In this subsection, it evaluates the performance of the suggested approach utilizing various methods, containing, Neural Network (NN),

Generative Adversarial Network (GAN), Recurrent Neural Network (RNN) and Leaky ReLU-GRU. The evaluation is conducted on the Noor Eye Hospital dataset, and results were represented in Table 5, Table 6, Table 7 and Table 8. Where, Table 5 represents the value obtained from the suggested method in Noor Eye Hospital dataset for Actual Features while Table 6 represents the Optimized features. Then, Table 8 represents the Different optimization algorithms. Finally, Table 8 represents Different activation functions were represented in below;

Table 5. Performance Analysis Of The Noor Eye Hospital Dataset For Actual Features

Actual Features	Accuracy	Sensitivity	Specificity	MCC	Error-rate
NN	86.64	85.55	87.87	84.06	13.36
GAN	86.47	85.88	83.82	84.72	13.53
RNN	92.72	89.67	88.84	90.87	7.28
LeakyRELU-GRU	94.98	93.92	95.64	92.43	5.02

The results from Table 5 demonstrate that the proposed method serves as an excellent classifier for distinguishing retinal patients in the Noor Eye Hospital dataset. The performance of the

suggested classification method outperforms the existing model in terms of overall metrics, particularly in the accuracy of 94.98% respectively.

Table 6. Performance Analysis Of Noor Eye Hospital Dataset For Optimized Features

Optimized Features	Accuracy	Sensitivity	Specificity	MCC	Error-rate
NN	87.89	88.22	89.86	90.65	12.11
GAN	87.42	88.01	86.98	89.03	12.58
RNN	93.91	90.40	91.62	92.87	6.09
LeakyRELU-GRU	99.59	99.79	98.28	96.47	0.41

The results from Table 6 demonstrate that the proposed method serves as an excellent classifier for distinguishing retinal patients in the Noor Eye Hospital dataset. The performance of the suggested classification methods outperforms the

existing model in terms of overall metrics, particularly in accuracy of 99.59% respectively. Table 6 evaluates the performance evaluation of the suggested approach utilizing various methods, containing, PSO, ACO, and ABC.

Table 7. Performance Analysis Of Noor Eye Hospital Dataset For Different Optimization Algorithms

Optimization methods	Accuracy	Sensitivity	Specificity	MCC	Error-rate
PSO	92.91	93.76	93.67	91.61	7.09
ACO	93.76	92.84	94.48	92.90	6.24
ABC	95.81	96.89	94.99	95.90	4.19
Proposed	99.59	99.79	98.28	96.47	0.41

The results from Table 7 demonstrate that the proposed method serves as an excellent classifier for distinguishing retinal patients in the Noor Eye Hospital dataset. The performance of the suggested classification methods outperforms the

existing model in terms of overall metrics, particularly in accuracy of 99.59% respectively. Table 8 evaluates the performance analysis of activation functions like Sigmoid, ReLU, Tanh, and Leaky ReLU-GRU.

Table 8 Performance Analysis Of Different Activation Functions

activation functions	Accuracy	Sensitivity	Specificity	MCC	Error-rate
Sigmoid	95.84	96.91	94.66	93.88	4.16
RELU	98.74	95.78	93.89	94.92	1.26
Tanh	93.39	92.72	90.89	91.72	6.61
LeakyRELU-GRU	99.59	99.79	98.28	96.47	0.41

The results from Table 8 demonstrate that the proposed method serves as an excellent classifier for distinguishing retinal patients in the Noor Eye Hospital dataset. The performance of the suggested classification methods outperforms the existing model in terms of overall metrics, particularly in accuracy of 99.59% respectively.

4.4. Comparative analysis

Comparative analysis refers to the comparison of data to identify similarities and differences for meaningful insights or decision-making. In this subsection, the classification approach performance is assessed by comparing it with existing approaches listed in related works. The values obtained from evaluating the proposed approach for the OCT images and Noor Eye Hospital dataset were represented in Table 9 and Table 10.

Table 9. Comparative Analysis Of Proposed Method For OCT Images Dataset

Methods	Accuracy (%)	Sensitivity (%)
DME [17]	95.70	98.00
CNN [18]	96.53	96.00
Proposed	99.01	99.16

The graphical representation of the comparative analysis for OCT dataset is illustrated in Figure 4.

Table 9 and Figure 4 describe how the suggested classification model outperformed existing models in overall performance metrics for the OCT images dataset. The accuracy achieved by the proposed approach is 99.1%, significantly higher than the Diabetic Muscular Edema (DME) of 95.70%, and Convolutional Neural Networks (CNN) of 96.53% respectively.

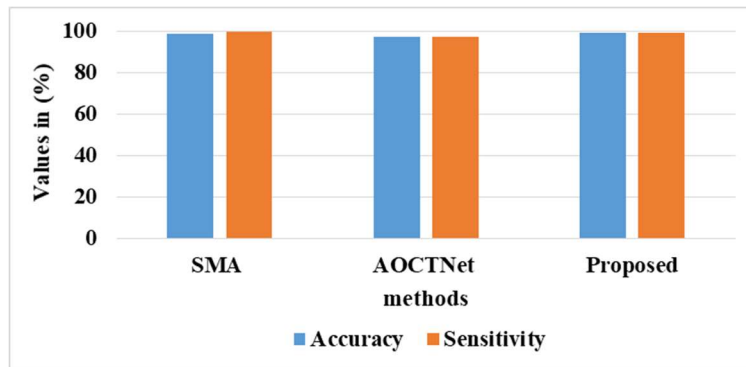


Figure 4. Graphical Image Of Comparative Evaluation For OCT Images Dataset

Table 10. Comparative Analysis Of The Proposed Method For Noor Eye Hospital Dataset

Methods	Accuracy (%)	Sensitivity (%)
SMA[16]	97.49	96.37
MSKξMP [19]	96.68	96.63
Proposed	99.59	99.79

The graphical representation of the comparative analysis for Noor Eye dataset is illustrated in Figure 5.

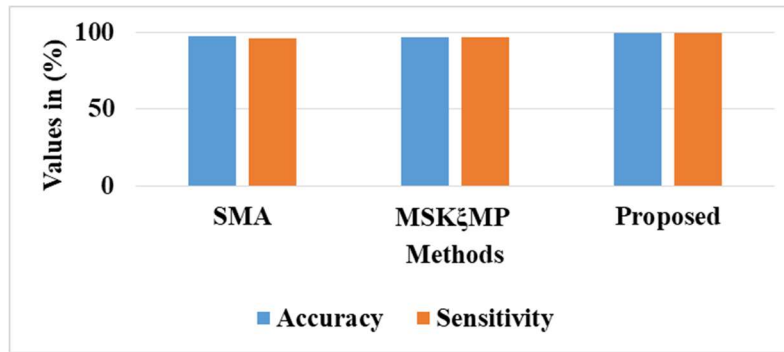


Figure 5. Graphical Image Of Comparative Evaluation For Noor Eye Dataset

4.5 Discussion

The effectiveness of the suggested method and the drawbacks of the existing approaches are discussed in this section. [16] increased training costs, and it is essential to conduct clinical validation in the experimental analysis to determine its effectiveness and reliability. [19] needs to be analyzed with activation layers for both test scenarios and adversarial situations for the decision-making process. To address these issues, the suggested method improves the performance and accuracy in retinal prediction. According to the results, the proposed technique attained a higher accuracy of 99.01% in the OCT image dataset and 99.59% accuracy on the Noor Eye dataset, which was greater than the existing approaches [16] [19] respectively.

5. CONCLUSION

The suggested Leaky ReLU-GRU method was utilized to generate a high-performance result for accurate retinal disease prediction in feature extraction and selection. Normalization techniques are used to pre-process input images, while GLCM and Local Ternary Patterns are used to extract features. The LMOA feature selection method improves model performance by selecting relevant features. Finally, a Leaky ReLU-GRU approach is

proposed for improving classification accuracy in retinal eye disease. According to the experimental results, the proposed method outperformed existing methods with an accuracy of 99.01% in the OCT images dataset and 99.59% in the Noor Eye dataset. The proposed approach has been shown to be effective in identifying patients, reducing image noises, and contributing to the overall improvement of retinal disease diagnosis. In the future, need to develop the algorithm to acquire higher accuracy with the use of additional optimization approaches.

REFERENCES:

- [1]. Rani BMS, Ratna VR, Srinivasan VP, Thenmalar S, Kanimozhi R. Disease prediction based retinal segmentation using bi-directional ConvLSTMU-Net. J. Ambient Intell. Hum. Comput. 2021 Mar 15.
- [2]. Karthiyayini R, Shenbagavadivu N. Retinal image analysis for ocular disease prediction using rule mining algorithms. Interdiscip. Sci.: Comput. Life Sci. 2021 Sep; 13(3):451-62.
- [3]. Müller D, Soto-Rey I, Kramer F. Multi-disease detection in retinal imaging based on ensembling heterogeneous deep learning models. In: German Medical Data Sciences

- 2021: Digital Medicine: Recognize–Understand–Heal. IOS Press; 2021. pp. 23-31.
- [4]. Fragiotta S, Abdolrahimzadeh S, Dolz-Marco R, Sakurada Y, Gal-Or O, Scuderi G. Significance of hyperreflective foci as an optical coherence tomography biomarker in retinal diseases: characterization and clinical implications. *J. Ophthalmol.* 2021 Dec; 2021:6096017.
- [5]. Li X, Hu X, Qi X, Yu L, Zhao W, Heng PA, Xing L. Rotation-oriented collaborative self-supervised learning for retinal disease diagnosis. *IEEE Trans. Med. Imaging* 2021 Apr 23; 40(9):2284-94.
- [6]. Lee J, Lee J, Cho S, Song J, Lee M, Kim SH, Lee JY, Shin DH, Kim JM, Bae JH, Song SJ. Development of decision support software for deep learning-based automated retinal disease screening using relatively limited fundus photograph data. *Electronics* 2021 Jan 13; 10(2):163.
- [7]. Tayal A, Gupta J, Solanki A, Bisht K, Nayyar A, Masud M. DL-CNN-based approach with image processing techniques for diagnosis of retinal diseases. *Multimedia Syst.* 2022 Aug; 28(4):1417-1438.
- [8]. Fadaie Z, Whelan L, Ben-Yosef T, Dockery A, Corradi Z, Gilissen C, Haer-Wigman L, Corominas J, Astuti GD, de Rooij L, van den Born LI. Whole genome sequencing and in vitro splice assays reveal genetic causes for inherited retinal diseases. *npj Genomic Med.* 2021 Nov 18; 6(1):97.
- [9]. Kim KM, Heo TY, Kim A, Kim J, Han KJ, Yun J, Min JK. Development of a fundus image-based deep learning diagnostic tool for various retinal diseases. *Journal of Personalized Medicine* 2021 Apr 21; 11(5):321.
- [10]. Zhang Q, Li J, Bian M, He Q, Shen Y, Lan Y, Huang D. Retinal imaging techniques based on machine learning models in recognition and prediction of mild cognitive impairment. *Neuropsychiatr. Dis. Treat.* 2021; 2021(17):3267-81.
- [11]. Parameswari C, Ranjani SS. Prediction of atherosclerosis pathology in retinal fundal images with machine learning approaches. *J. Ambient Intell. Hum. Comput.* 2021 Jun; 12(6):6701-11.
- [12]. Yanagihara RT, Lee CS, Ting DSW, Lee AY. Methodological challenges of deep learning in optical coherence tomography for retinal diseases: a review. *Transl. Vision Sci. Technol.* 2020 Feb; 9(2):11.
- [13]. Sengar N, Joshi RC, Dutta MK, Burget R. EyeDeep-Net: A multi-class diagnosis of retinal diseases using deep neural network. *Neural Computing and Applications* 2023 May; 35(14):10551-71.
- [14]. Mohammad, A, Utso, MZ, Habib, SB and Das, AK. Predicting Retinal Diseases using Efficient Image Processing and Convolutional Neural Network (CNN). *Journal of Engineering Advancements* 2021 Dec 27; 2(04):221-7.
- [15]. Aoun M, Passerini I, Chiurazzi P, Karali M, De Rienzo I, Sartor G, Murro V, Filimonova N, Seri M, Banfi S. Inherited Retinal Diseases Due to RPE65 Variants: From Genetic Diagnostic Management to Therapy. *International Journal of Molecular Sciences.* 2021 Jul 5; 22(13):7207.
- [16]. Toğaçar, M, Ergen, B, Tümen, V. Use of dominant activations obtained by processing OCT images with the CNNs and slime mold method in retinal disease detection. *Biocybern. Biomed. Eng.* 2022 Apr-Jun; 42(2):646-66.
- [17]. Alqudah A, Alqudah AM, AlTantawi M. Artificial intelligence hybrid system for enhancing retinal diseases classification using automated deep features extracted from OCT images. *Int. J. Intell. Syst. Appl. Eng.* 2021 Sep 24; 9(3):91-100.
- [18]. Xu L, Wang L, Cheng S, Li Y. MHANet: A hybrid attention mechanism for retinal diseases classification. *Plos one* 2021 Dec 16; 16(12):e0261285.
- [19]. Liew A, Agaian S, Benbelkacem S. Distinctions between Choroidal Neovascularization and Age Macular Degeneration in Ocular Disease Predictions via Multi-Size Kernels ξ cho-Weighted Median Patterns. *Diagnostics.* 2023 Feb 14; 13(4):729.
- [20]. Kim J, Tran L. Retinal disease classification from OCT images using deep learning algorithms. 2021 IEEE Conference on Computational Intelligence in Bioinformatics and Computational Biology (CIBCB), Melbourne, Australia. IEEE; 2021. pp. 1-6.
- [21]. Pritoonka AK, Kiani F. Texture image analysis based on joint of multi directions GLCM and local ternary patterns. arXiv preprint arXiv:2209.01866 2022.